Semiconductor Physics, Quantum Electronics & Optoelectronics, 2024. V. 27, No 1. P. 010-027.

Semiconductor physics

Space charge region recombination in highly efficient silicon solar cells

A.V. Sachenko[1*], V.P. Kostylyov[1], M. Evstigneev[2]

[1]*V. Lashkaryov Institute of Semiconductor Physics, NAS of Ukraine, 41, prosp. Nauky, 03680 Kyiv, Ukraine*
[2]*Department of Physics and Physical Oceanography, Memorial University of Newfoundland, St. John's, NL, A1B 3X7 Canada*
[*]*Corresponding author e-mail: sach@isp.kiev.ua*

Abstract. The recombination rate in the space charge region (SCR) of a silicon-based barrier structure with a long Shockley–Reed–Hall lifetime is calculated theoretically by taking into account the concentration gradient of excess electron-hole pairs in the base region. Effects of the SCR lifetime and applied voltage on the structure ideality factor have been analyzed. The ideality factor is significantly reduced by the concentration gradient of electron-hole pairs. This mechanism provides an increase of the effective lifetime compared to the case when it is insignificant, which is realized at sufficiently low pair concentrations. The theoretical results have been shown to be in agreement with experimental data. A method of finding the experimental recombination rate in SCR in highly efficient silicon solar cells (SCs) has been proposed and implemented. It has been shown that at the high excess carrier concentration exceeding 10^{15} cm^{-3} the contribution to the SCR recombination velocity from the initial region of SCR that became neutral is significant. From a comparison of theory with experiment, the SCR lifetime and the ratio of the hole to the electron capture cross sections are determined for a number of silicon SCs. The effect of SCR recombination on the key characteristics of highly efficient silicon SCs, such as photoconversion efficiency and open-circuit voltage, has been evaluated. It has been shown that they depend not only on the charge carrier lifetime in SCR, but also on the ratio of hole to electron capture cross sections σ_p/σ_n. When $\sigma_p/\sigma_n < 1$, this effect is significantly strengthened, while in the opposite case $\sigma_p/\sigma_n > 1$ it is weakened. It has been ascertained that in a number of highly efficient silicon SCs, the distribution of the inverse lifetime in SCR is described by the Gaussian one. The effect described in the paper is also significant for silicon diodes with a thin base, *p-i-n* structures, and for silicon transistors with *p-n* junctions. In Appendix 2, the need to take into account the lifetime of non-radiative excitonic Auger recombination with participation of deep impurities in silicon is analyzed in detail. It has been shown, in particular, that considering it enables to reconcile the theoretical and experimental dependences for the effective lifetime in the silicon bulk.

Keywords: silicon solar cell, space charge region recombination, open-circuit voltage, short-circuit current, photoconversion efficiency.

https://doi.org/10.15407/spqeo27.01.010
PACS 88.40.hj, 88.40.jj

Manuscript received 18.12.23; revised version received 08.01.24; accepted for publication 28.02.24; published online 12.03.24.

1. Introduction

More than 60 years have passed since the publication of the classic study [1] of the recombination rate in the *p-n* junction space charge region (SCR). After this publication, physicists actively published works in which various aspects of this problem were considered [2–7]. But even in the 21st century, this subject has not yet been fully exhausted (see, for example, Ref. [8]).

An approximate analysis of the generation-recombination processes in the depletion layer is given in the monograph [9]. It is based on the assumption that the quasi-Fermi levels of both charge carrier types are constant in SCR. Examination of the expression for the Shockley–Reed–Hall (SRH) recombination rate shows that the maximum value of the recombination rate corresponds to the position where the intrinsic Fermi energy, E_{Fi}, is equally distant from the quasi-Fermi levels of electrons and holes. On both sides of the maximum, the recombination rate decreases exponentially with the characteristic length kT/qE, where E is the electric field strength in SCR, q is the elementary charge, k is Boltzmann's constant, T is absolute temperature, and kT is the thermal energy. The effective thickness

of the recombination region can be represented as $2kT/qE = kTw_d/q(V_d - V)$, where w_d is the depletion region thickness, V_d is the built-in voltage and V is the applied voltage. From this analysis, the authors [9] conclude that for a spatially homogeneous distribution of recombination centers, the diode ideality factor n is always less than two.

In the work [1] this issue was analyzed more thoroughly for a symmetrical *p-n* junction. It was established that the diode ideality factor is a function of the recombination center energy E_t, the temperature T, and the applied voltage V, and its maximum value is equal to 1.8 when $E_t \approx E_i$.

Choo [4] improved the theory [1] for the case of asymmetric junctions, in which the lifetimes of electrons τ_{n0} and holes τ_{p0} can vary in a wider range. As compared to the classical theory [1], the analysis performed in [4] gives smaller generation-recombination currents, which reach saturation at the high forward bias. The values of ideality factor can be both smaller and larger than 2.

In [10], a more complex and more accurate model was developed as compared to the Sah–Noise–Shockley (SNS) model [1]. It differs from the SNS model in two aspects. First, the potential $\psi(x)$ is found from the Poisson equation. Second, the depletion approximation is not used to determine the thickness w_d of SCR; rather, the integration limits were defined from the condition $d\psi(x)/dx = 0$.

In [11], an analytical method for calculating the recombination current in the depletion region of a forward-biased diode with an abrupt junction was proposed. The method uses the SRH recombination approximation through one energy level, the concentration of which does not vary much depending on the position in SCR. This model is systematically compared with previous models and with the results of numerical calculations using PC-1D software. It has been shown that the proposed method [11], despite its simplicity, gives results closer to PC-1D numeric simulation than previous models. In addition, it has been shown that the Nussbaum model [10] can be better agreed with the numerical results by reducing the integration limits by $0.3kT$.

The DESSIS semiconductor device simulation program was used in [12] to model the recombination current and determine the ideality factor. With this aim, a complete set of differential equations for semiconductors was solved without using the aforementioned approximations. Numerical modeling of DESSIS was used to determine the most accurate values of ideality factor and compare with them theoretical models, in particular [10, 11]. At the same time, it was shown that the Nussbaum model [10] gives results sufficiently close to the results of numerical simulation.

It should be noted that the ideality factor of silicon diodes at low applied voltages is not always related to the SCR recombination. Firstly, the initial region of the *I–V* characteristic is usually defined by the shunt resistance, so the ideality diode factor in the voltage range up to 0.3 V can significantly exceed two. Secondly, in silicon diodes or *p-n* junction barrier structures with sufficiently long bulk lifetimes on the order of or longer than 1 ms, there is another physical mechanism that provides an ideality factor of 2. Namely, when the excess concentration Δn significantly exceeds the level of doping, *i.e.* $\Delta n >> N_d$ (for definitness, we will consider an *n*-type semiconductor), the activation energy becomes comparable to half the bandgap, $E_a \approx E_g/2$, and the value of the ideality factor $n \approx 2$. This is exemplified by the heterostructure from [10], in which the ideality factor has the value of 1.8 at the applied voltage V ranging from 0.4 to 0.65 V.

In this work, the physical mechanism that ensures reduction of the ideality factor compared to the value $n = 2$ in silicon *p-n* junction structures with long bulk lifetimes of charge carriers is discussed. It is operative at sufficiently high recombination rates in SCR and is related to the concentration gradient of excess electron-hole pairs in the bulk of semiconductor. The condition for the emergence of this gradient is a large difference in the recombination velocities on the opposite different surfaces. Namely, on the surface with a *p-n* junction, the high net recombination rate is related to the SCR recombination, especially at low excitation levels. On the opposite surface that has no SCR, the total recombination rate is significantly lower. In its pure form, this mechanism manifests itself when the diffusion length significantly exceeds the thickness of the structure (more precisely, its base region) d. It is shown that this mechanism provides an increase in the effective lifetime of excess electron-hole pairs as compared to the case when it is insignificant, which is realized at sufficiently low values of Δn. A method is proposed to determine experimentally the recombination rate in SCR in silicon p^+-n-n^+ structures. It is shown that at high excess carrier concentration exceeding 10^{15} cm^{-3} the contribution to the SCR recombination velocity from the initial region of the SCR that became neutral is significant.

The classification of the effect of SCR recombination on the key characteristics of highly efficient silicon SCs, depending on the minority charge carrier lifetime τ_R in SCR, is performed. The results of works [14, 15] were used, in which it was established that the lifetime in SCR is significantly shorter than the SRH lifetime in the base region and can be of the order of or less than one microsecond.

A similar situation occurs during passivation of silicon with the SiN_x layers (see, for example, [16]), when a significant positive static fixed charge gets built-in into the dielectric. Then, the conductivity inversion occurs near the *p*-type silicon surface, and the SCR recombination becomes significant. In the work [16], lifetimes of the order of one microsecond were also observed in SCR.

2. Expressions for the SCR recombination velocity in the presence of excess carrier concentration gradient in the bulk semiconductor

We will consider the case when the SCR recombination is determined by a single deep impurity level, filling of which is described by the SRH statistics. Then, the value of the recombination velocity can be found by integrating the inverse recombination lifetime $\tau_R^{-1}(x)$ over the SCR thickness w:

$$S_{SC} = \int_0^w \frac{\tau_R^{-1}(x)(n_0+\Delta n)dx}{(n_0+\Delta n)e^{y(x)} + n_i(T)e^{E_t/kT} + b_r\left((p_0+\Delta n)e^{-y(x)} + n_i(T)e^{-E_t/kT}\right)}. \quad (1)$$

Here, $y(x)$ is the electric potential in SCR divided by the thermal voltage kT/q, n_0 and p_0 are the equilibrium electron and hole concentrations, $p_0 = n_i(T)^2/n_0$, $n_i(T)$ is the intrinsic carrier concentration, Δn is the excess carrier concentration and $b_r = C_p/C_n$ is the ratio of the hole and electron capture coefficients, which are expressed in terms of the respective thermal velocities, $V_{n,p}$, and capture cross-sections, $\sigma_{n,p}$, as $C_{n,p} = V_{n,p}\,\sigma_{n,p}$.

Almost all works devoted to the calculation of the recombination rate in the SCR analyze the case when the SCR recombination time $\tau_R(x) = \text{const}$. Changing the integration variable from the coordinate x to the dimensionless potential y, we obtain

$$S_{SC}(\Delta n) = \int_{y_w}^{y_0} \frac{\tau_R^{-1}(n_0+\Delta n)dy}{(n_0+\Delta n)e^{y} + n_i(T)e^{E_t/kT} + b_r\left((p_0+\Delta n)e^{-y} + n_i(T)e^{-E_t/kT}\right)} F(y), \quad (2)$$

where

$$F(y) = \frac{L_D}{\left(\frac{n_0+\Delta n}{n_0}\left(e^{y}-1\right) + y + \frac{p_0+\Delta n}{n_0}\left(e^{-y}-1\right)\right)^{1/2}}. \quad (3)$$

Here, $L_D = \left(\varepsilon_0\varepsilon_{Si}kT/2q^2n_0\right)^{1/2}$ is the Debye length, q is the elementary charge, y_0 is the non-equilibrium non-dimensional band bending value on the surface of the weakly doped region, which depends on the injection level Δn and is found from the integral neutrality condition, and y_w is the non-equilibrium non-dimensional potential on the boundary between the SCR and the quasi-neutral region.

The dependence of the non-equilibrium dimensionless potential y on the coordinate x is found from the Poisson equation:

$$x = \int_{y_0}^{y} \frac{L_D}{\left(\frac{n_0+\Delta n}{n_0}\left(e^{y_1}-1\right) - y_1 + \frac{\Delta n}{n_0}\left(e^{-y_1}-1\right)\right)^{1/2}} dy_1. \quad (4)$$

The value of the non-equilibrium dimensionless potential y_0 at $x = 0$ is found from the solution of the integral electric neutrality equation, which has the form

$$N = \pm\left(\frac{2kT\varepsilon_0\varepsilon_{Si}}{q^2}\right)^{1/2} \sqrt{\left[\begin{array}{l}(n_0+\Delta n)\left(e^{y_0}-1\right) - \\ -n_0y_0 + \Delta n\left(e^{-y_0}-1\right)\end{array}\right]}, \quad (5)$$

where qN is the surface charge density of acceptors in the p-n junction or in an anisotypic heterojunction.

The simplest expression for the recombination velocity in SCR is obtained for the case of a small excitation level $\Delta n << n_0$, and the recombination level is located in the middle of the band gap. In this case, the integrand in the equation (2) has a symmetric bell-shaped character and can be integrated over y up to the maximum point $y_m = (1/2)\ln\left[n_0/b_r\left(n_i(T)^2/n_0 + \Delta n\right)\right]$. Then we get

$$S_{SC}^{an}(\Delta n) \approx \frac{kL_D}{\tau_R}\frac{\exp(y_m)}{\sqrt{y_m}}, \quad (6)$$

where k is a numerical coefficient of the order of 2.

The expression (6) can be used to calculate the value of S_{SC}, if $y_m > 2$. It should be noted that it does not apply near the point of maximum power collection of a silicon p-n junction SC, because in this case the criterion $y_m > 2$ is not fulfilled. It breaks down especially early when $b_r > 1$. As for the expression (2), it allows finding the recombination velocity in the SCR numerically at any ratio $\Delta n/n_0$.

This paper considers the case when the SRH lifetime in silicon is greater than 1 ms. In this case, the diffusion length significantly exceeds the thickness of the SC base region, *i.e.* the inequality $L >> d$ holds, where $L = \left(D\tau_{eff}^b\right)^{1/2}$. Here, D is the diffusion coefficient of excess electron-hole pairs, and τ_{eff}^b is the effective lifetime of charge carriers in the base region. The excess concentration of charge carriers in the base is constant when the criterion $S_{sum} << D/d$ is fulfilled, where S_{sum} is the total recombination rate in the SCR and on the front and rear surfaces of the base region of the semiconductor barrier structure of the thickness d. If this criterion is not fulfilled due to the fact that the rate of recombination on one of the surfaces of the base is significantly greater

than the rate of recombination on another surface, then the Δn value will depend on the x coordinate. This case is realized at low levels of excitation precisely due to recombination in SCR.

Let us first consider the situation when the SCR recombination occurs on the back surface at $x = d$. The generation-recombination balance equation in this case has the following form:

$$J_{SC} = q\left[\int_0^d \frac{\Delta n(x)dx}{\tau_{eff}^b(x)} + S_0\Delta n(0) + S_{SC}\Delta n(d) + S_d\,\Delta n(d)\right], \quad (7)$$

where J_{SC} is the short-circuit current density, which is approximately equal to photocurrent J_L, $J_{SC} \cong J_L$, τ_{eff}^b is the effective bulk lifetime in the base, S_0 is the effective surface recombination velocity at $x = 0$, S_d is the effective surface recombination velocity at $x = d$, and S_{SC} is the recombination velocity in SCR on the back surface.

In order to find the distribution of excess charge carriers with the coordinate x, which is perpendicular to the surface, we will look for a solution of the diffusion equation in the form:

$$\Delta n(x) = C_1\exp\left(-\frac{x}{L}\right) + C_2\exp\left(\frac{x}{L}\right). \quad (8)$$

To determine the coefficients C_1 and C_2, we will use the following boundary condition on the front surface:

$$\Delta n(x=0) = C_1 + C_2 \quad (9)$$

and on the back surface:

$$S_{SC}\left(C_1e^{-d/L} + C_2e^{d/L}\right) = \frac{D}{L}\left(C_1e^{-d/L} - C_2e^{d/L}\right). \quad (10)$$

In a general case,

$$C_2 = C_1\frac{(D/L - S_{SC})e^{-d/L}}{(D/L + S_{SC})e^{d/L}}. \quad (11)$$

Using (9) and (11), we obtain

$$\Delta n(x=0) \cong C_1\left(1 + \frac{D/L - S_{SC}}{D/L + S_{SC}}\exp\left(-\frac{2d}{L}\right)\right). \quad (12)$$

In a similar manner, we obtain a relation between $\Delta n(x = d)$ and C_1

$$\Delta n(x=d) = C_1\frac{D}{L}\cdot\frac{\left(1+e^{-d/L}\right) + S_{SC}\left(1-e^{-d/L}\right)}{(D/L + S_{SC})e^{d/L}}. \quad (13)$$

In this paper, we will limit ourselves to the case Δn = const. This approximation is also valid when the rates of bulk and surface recombination are significantly lower than the rate of recombination in SCR, because their contribution can be neglected then. Taking into account the expressions (12) and (13) in (7), we get

$$J_{SC} = q\left[\frac{d}{\tau_{eff}^b(x=0)} + S_0 + b_dS_{SC} + S_d\right]\Delta n(x=0), \quad (14)$$

where the parameter b_d is found from the equation:

$$b_d = \frac{2(D/L)e^{-d/L}}{D/L + b_dS_{SC}(\Delta n) + (D/L - b_dS_{SC}(\Delta n))e^{-2d/L}},$$

$$\text{or} \quad b_d = \frac{1}{\cosh\left(\frac{d}{L}\right) + S_{SC}b_d\frac{L}{D}\sinh\left(\frac{d}{L}\right)} \quad (15)$$

and $S_{SC}(\Delta n)$ is determined by (2).

As can be seen from (14), in this case it is possible to introduce an effective SCR recombination velocity

$$S_{SCd} = b_dS_{SC}(\Delta n). \quad (16)$$

Similarly, we can consider the case when the SCR exists on the surface $x = 0$. In this case, the recombination-generation balance equation has the form

$$J_{SC} = q\left[\frac{d}{\tau_{eff}^b(x=d)} + S_0 + b_0S_{SC} + S_d\right]\Delta n(x=d), \quad (17)$$

where the coefficient b_0 is given by

$$b_0 = 2\frac{D}{L}\cdot\frac{e^{d/L}}{D/L - b_0S_{SC}(\Delta n) + (D/L + b_0S_{SC}(\Delta n))e^{2d/L}}$$

$$\text{or} \quad b_0 = \frac{1}{\cosh\left(\frac{d}{L}\right) + S_{SC}b_0\frac{L}{D}\sinh\left(\frac{d}{L}\right)}. \quad (18)$$

In the same way as before, it is possible to introduce the effective SCR recombination velocity on the surface $x = 0$:

$$S_{SC0} = b_0S_{SC}(\Delta n). \quad (19)$$

To demonstrate the dependence of the excess concentration on the x-coordinate, let us consider a simpler case where the recombination velocity on the back surface is determined by the surface recombination. In this case, the spatial dependence of the excess carrier concentration is

$$\Delta n(x) = \Delta n(x=0)\left(e^{-x/L} + \frac{D/L - S_{deff}}{D/L + S_{deff}}e^{x/L}\right),$$

where $S_{deff} = b_{ds}S_d$, and

$$b_{ds} = 2\frac{D}{L}\cdot\frac{e^{-d/L}}{D/L + S_d + (D/L - S_d)e^{-2d/L}}. \quad (20)$$

Shown in Fig. 1a is the dependence of the excess carrier concentration in the base on the x coordinate, obtained from (20) by using the following parameters: $\tau_{SRH} = 10^{-2}$ s, $d = 1.5\cdot10^{-2}$ cm, $L = 0.33$ cm of the back surface. The curves are parameterized by the back surface recombination velocity, which for the case of curves *1*–*6*, respectively, was assumed equal to 1, 10, 10^2, 10^3, 10^4, and 10^5 cm/s.

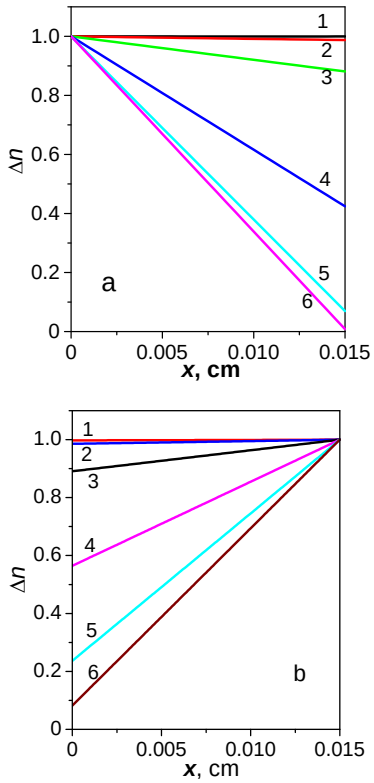

Fig. 1. Excess carrier concentration as a function of coordinate x in the case when the surface recombination velocity on (a) the back surface and (b) the front surface is set to 1 (*1*), 10 (*2*), 10^2 (*3*), 10^3 (*4*), 10^4 (*5*), and 10^5 cm/s (*6*).

As it can be seen from Fig. 1a, the excess concentration of minority carriers in the base changes linearly with x. At $S_d \leq 10$ cm/s, it changes weakly, in particular, for $S_d = 10$ cm/s, Δn decreases by one percent. In the case when $S_d = 10^4$ cm/s, it decreases by more than an order of magnitude, and when $S_d = 10^5$ cm/s, it varies by approximately two orders of magnitude.

Fig. 1b shows the dependence $\Delta n(x)$ for the case when the surface recombination rate S_0 is high on the frontal surface $x = 0$. As can be seen from the figure, in this case the value of $\Delta n(x)$ decreases according to a linear law when approaching the surface at $x = 0$. Although the dependences shown in Figs 1a and 1b are symmetrical, Fig. 1b is interesting in that, despite the fact that the light is absorbed by the semiconductor from the side of front surface, the concentration of excess pairs decreases when approaching it. This dependence is completely controlled by the value of the surface recombination velocity on this surface.

As can be seen from the comparison of (15) and (18), the expressions for b_0 and b_d are identical. Therefore, their dependence on the value of τ_R coincide, as it can be seen from Fig. 2. This figure shows the dependence of coefficients b_0 and b_d on the value of τ_R. As it can be seen from the figure, these two curves coincide and decrease by almost an order of magnitude as the lifetime decreases within the specified range. Note

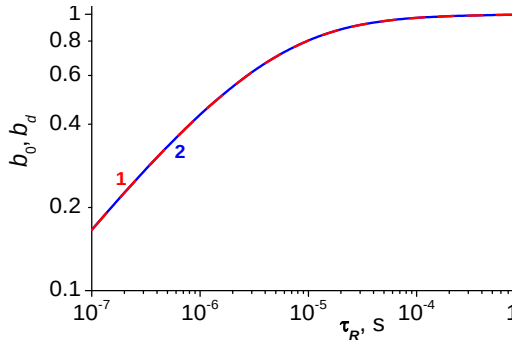

Fig. 2. The coefficients b_0 (*1*) and b_d (*2*) that describe a decrease in the effective SCR recombination velocity on the charge carrier lifetime in the base region.

that the SCR recombination is active on the rear surface in silicon SCs based on the structures with rear metallization (see [17, 18]), while in the structures with a conventional geometry it is operative on the front surface (see work [13, 14]).

The magnitude of the SCR recombination velocity is primarily influenced by the value of the SCR lifetime τ_R, the ratio of hole and electron capture cross sections b_r and the doping level n_0. It increases with decreasing values of τ_R and b_r and increases with increasing n_0. The value of SCR lifetimes τ_R for different rectifying structures varies widely, usually from 10^{-4} down to 10^{-7} s, and is three to four orders of magnitude smaller than the SRH lifetime in the neutral volume. We will not discuss the reason for this difference now, but will accept it as an experimental fact [14–16].

Fig. 3 shows the calculated theoretical dependences of the recombination velocity in SCR on the excess concentration of electron-hole pairs Δn for SC with the carrier lifetime in SCR that differs by an order of magnitude (10^{-6} s (a) and 10^{-7} s (b)). Curves *1* and *2* illustrate the dependence of S_{SC0} and S_{SCd} on Δn, respectively. Curve *3* represents the dependence of $S_{SC}(\Delta n)$, and curve *4* in Fig. 3a is an approximation to $S_{SC}(\Delta n)$ in the form of $S_a \sim \Delta n^{-0.6}$.

Fig. 4 shows the ideality factor related to the SCR recombination

$$n = \frac{q}{kT}\left(\frac{d\ln(J)}{dV}\right)^{-1}, \tag{21}$$

$$J = qS_{SCd}(\Delta n)\Delta n,$$

$$\Delta n(V) = -\frac{n_0}{2} + \sqrt{\left(\frac{n_0}{2}\right)^2 + n_i(T)^2\left(e^{qV/kT} - 1\right)}, \tag{22}$$

vs. the SCR lifetime in silicon barrier structures. The parameter of the curves is b_r, *i.e.* the ratio of the hole-to-electron capture cross sections. Fig. 4 shows that the value of n is always less than 2; its minimum value is close to 1.3. The reduction of the ideality factor begins at significantly longer SCR lifetimes than the reduction of the coefficients b_d or b_0.

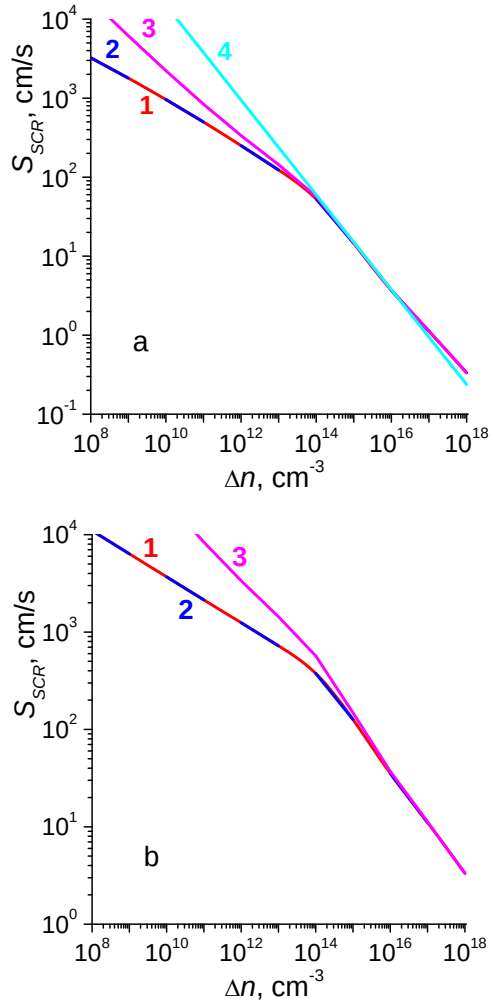

Fig. 3. The effective SCR recombination velocity dependent on the excitation level for the SCR lifetime set to 10^{-6} s (a) and 10^{-7} s (b). The curves *1* and *2* describe S_{SC0} and S_{SCd} *vs.* Δn, the curve *3* shows $S_{SC}(\Delta n)$, and the curve *4* in panel (a) is an approximation of the form $S_a \sim \Delta n^{-0.6}$.

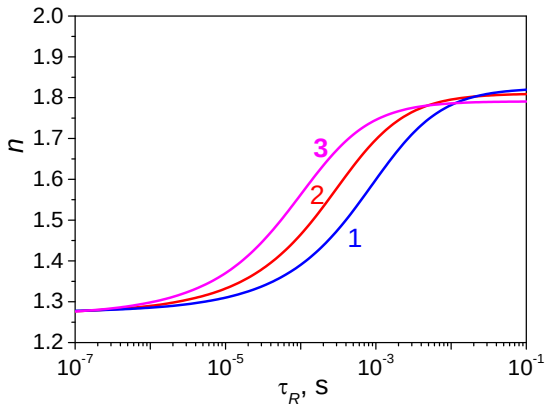

Fig. 4. The ideality factor associated with the SCR recombination as a function of the lifetime of charge carriers in the base. The curves differ in the ratio of hole and electron capture cross sections: $b_r = 0.1$, 1 and 10, respectively, for blue (*1*), red (*2*), and crimson (*3*) curves.

It can also be seen from Fig. 4 that the larger the value of the hole capture coefficient compared to the electron capture coefficient, the higher the values of the ideality factor for SCR.

As numerical estimates show, at $V = 0.1$ V, for typical parameters of silicon barrier structures with long lifetimes, the value of J is about 10^{-8} A/cm^2, while the current density, which is determined by the shunt resistance at its value of $3\cdot10^4$ Ohm·cm^2, equals $3\cdot10^{-6}$ A/cm^2. In order for the contribution from the SCR recombination current density to dominate, the value of the shunt resistance should be at least three orders of magnitude larger. Since the following theoretical approach will be applied to the structures mentioned above, and in them the shunt resistance values lie within the range from 10^3 up to 10^5 Ohm·cm^2, this circumstance must be taken into account.

We described the curves in Fig. 4 in such detail to show that the ideality factor due to SCR recombination in this case depends on several parameters and variables, in particular, the SCR lifetime, the ratio of the hole and electron capture cross sections, the excess concentration of electron-hole pairs, *etc*. Therefore, its value can be given only for illustrative purposes. As for the effect of SCR recombination on the characteristics of silicon structures, it should be investigated by analyzing, first of all, the dependence of SCR recombination velocity on the parameters mentioned above.

In simulation programs of a sufficiently high level, the ideality factor is not used, but the problem is solved being based on general equations, so the question of the ideality factor value does not arise (see, for example, the program PC-1d and its subsequent versions).

Unless stated otherwise, the following parameters will be used in the numerical evaluations and in the construction of the curves: $\tau_{SRH} = 10^{-2}$ s, $d = 150$ μm, $n_0 = 10^{15}$ cm^{-3}, $T = 300$ K.

At the end, we formulate the criteria for the validity of the results presented in the paper [1]. The first condition is the requirement that the thickness of the base region d significantly exceeds the diffusion length L. In this case, only one surface is involved and $\Delta n = \Delta n(x = 0)$. The second condition is the requirement that the excess concentration of electron-hole pairs Δn be much lower than the equilibrium concentration of the majority charge carriers n_0. In this case, the integral function in expression (1) is not significantly deformed due to Δn and the value of the non-ideality coefficient is close to 2. In most cases, the mentioned criteria are fulfilled for barrier structures based on all semiconductors except modern silicon. But in Ref. [15], we considered the samples of silicon SCs, for which these criteria are fulfilled. Fig. 5 shows the ideality factor as a function of the applied voltage for two SCs, one with a *n*-type base and the other with a *p*-type base, in which the diffusion lengths are much shorter than the thickness of the base (diffusion lengths are 166 and 50 μm, respectively, and the base thickness equals to 380 and 350 μm).

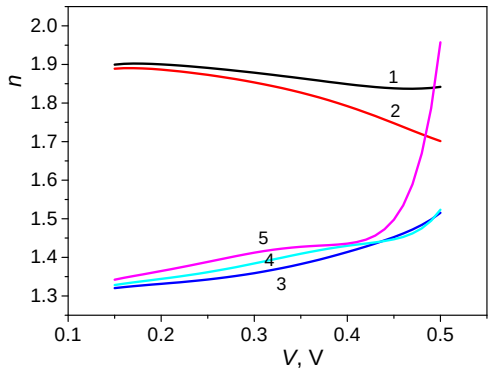

Fig. 5. The ideality factor of a *p-n* junction diode *vs*. applied voltage in a silicon structure with short (*1*, *2*) and long (*3–5*) diffusion length. The parameters used to build curves *1* and *2* are as follows: d_1 = 350 μm, $n_{01} = 3\cdot10^{15}$ cm^{-3}, L_1 = 50 μm, $\tau_{R1} = 1.2\cdot10^{-8}$ s, (*1*), d_2 = 380 μm, $n_{02} = 3.1\cdot10^{15}$ cm^{-3}, L_2 = 166 μm, $\tau_{R2} = 1.2\cdot10^{-6}$ s (*2*), T = 300 K. The curves *3–5* are built with the following parameter values d = 0.015 cm, L = 0.33 cm, $n_0 = 10^{15}$ cm^{-3}, T = 300 K, $N = 10^{12}$ cm^{-2}, $\tau_R = 5\cdot10^{-7}$ s (*3*), $5\cdot10^{-6}$ s (*4*) and $5\cdot10^{-5}$ s (*5*), respectively.

Fig. 5 also shows for comparison the theoretical curves for the ideality factor of SCR recombination on the applied voltage for a highly-efficient silicon SC sample, in which the diffusion length is an order of magnitude longer than the base thickness (respectively, 1800 and 150 μm). The parameter of the curves is the b_r value. As can be seen from the given figure, in this case, for SCs with short diffusion lengths, there is a weak dependence on the applied voltage, the values of the ideality factor are close to 2 and do not decrease significantly with increasing voltage. At the same time, the values of the ideality factor for SCs with a large diffusion length behave in accord with the theory outlined above, increasing from small values of the order of 1.3 to those higher than 1.4 at V = 0.4 V. If for the former, the values of the ideality factor decrease by 3% and 5% in the specified voltage range, then for the latter, they increase by 8% on average.

As compared to other semiconductors, monocrystalline silicon has a very long Shockley–Reed–Hall lifetime that can reach values around 100 ms. Although this material is mainly used to make solar cells, it can be applied for designing the diodes with a thin base and *p-i-n* structure. Therefore, the effects discussed in this work are also important for microelectronic devices based on monocrystalline silicon.

3. Experimental determination of $S_{SCd}(\Delta n)$ in silicon barrier structures

In this section, we will describe the theoretical basis of the method for experimentally determining the surface recombination velocity $S_{SCd}(\Delta n)$ as a function of the excess concentration and apply it in practice. For its implementation, it is necessary to subtract the contribution associated with all other recombination mechanisms from the total effective lifetime of charge carriers. The contribution from radiative recombination and interband Auger recombination is known and does not change from sample to sample, while the contribution from SRH recombination and from surface recombination must be determined using the known methods of their investigation, or by varying their values, fit experimental and theoretical dependences of $J_L(V_{OC})$. For a complete fit, it is necessary to pre-set the values of τ_R and b_R, which allows to find approximately the values of τ_{SRH} and S. When performing this procedure, it is expedient to set the initial value of b_R to unity.

This was done first by using the experimental dependences for the short-circuit current density on the applied voltage $J_L(V_{OC})$, described in our work [18]. The experimental dependence of $S_{SC}(\Delta n)$ defined in this way is shown in Fig. 6 (symbols).

To compare the obtained experimental dependence with the theory, two circumstances should be taken into account. First, in the cases where the value τ_R is small enough, in the region of sufficiently large values of Δn, in addition to SCR recombination, it is necessary to take into account the bulk recombination in that part of the SCR that has become neutral. Second, the model with τ_R = const is not realistic at medium and large excess concentrations. Much better is the model that describes the dependence of τ_R^{-1} on the x-coordinate in SCR by a Gaussian

$$\tau_R^{-1}(x) = \tau_{Rm}^{-1}\exp\left(-\frac{(x-x_m)^2}{2\sigma^2}\right), \qquad (23)$$

in which x_m is the position of the maximum, σ is the variance, τ_{Rm} is the lifetime at the maximum, The SCR recombination velocity becomes

$$S_{eff}^{SC} = \int_0^{d_{eff}} \frac{\tau_{Rm}^{-1}\exp\left(-\frac{(x-x_m)^2}{2\sigma^2}\right)(n_0+\Delta n)dx}{(n_0+\Delta n)e^{y(x)} + b_r(p_0+\Delta n)e^{-y(x)}}. \qquad (24)$$

The effective thickness d_{eff} is found from

$$\tau_{Rm}^{-1}\exp\left(-\frac{(d_{eff}-x_m)^2}{2\sigma^2}\right) = \tau_{SRH}^{-1}. \qquad (25)$$

It is the effective SCR thickness, up to which integration should be performed to correctly calculate S_{eff}^{SC}. The reason is that the experimental SCR lifetimes are lower than the SRH lifetime by a few orders of magnitude. Therefore, increasing the upper integration limit even by several times has very little effect on the value of obtained SCR recombination velocity.

The next problem is finding the SCR recombination velocity with account of the excess concentration gradient Δn. Previously, we used the following expression

$$b_d = \frac{1}{\cosh\left(\frac{d}{L}\right) + S_{SC}(\Delta n)b_d\frac{L}{D}\sinh\left(\frac{d}{L}\right)}. \qquad (26)$$

The value of $S_{SC}(\Delta n)$ in this equation is defined by the expression (2) and depends on the value of y_l, the dimensionless potential at the boundary of SCR and the quasi-neutral region. Note that the expression (2) enables to find the recombination velocity only in that part of SCR, where the magnitude of non-dimensional potential is higher than or equal to unity. By contrast, the expression (25) gives the total recombination velocity both in that part of SCR, where the electrostatic potential is higher than or equal to unity, and in that part, where the band straightening took place. At sufficiently large excess concentrations, the second term may exceed the first one. With account of it, the expression (26) should be generalized by replacing the value of $S_{SC}(\Delta n)$ with S_{sum}^{SC}.

The parameter $b_{d\,sum}$ that describes the ratio of excess concentrations on the surfaces $x = 0$ and $x = d$ in this case is defined as

$$b_{d\,sum} = \frac{1}{\cosh\left(\frac{d}{L}\right) + S_{sum}^{SC} b_{d\,sum} \frac{L}{D} \sinh\left(\frac{d}{L}\right)}. \qquad (27)$$

The quantity $S_{eff\,d}^{SC}$, which takes into account the gradient effect including the contribution from the region where the bands are straightened, is now found from

$$S_{eff\,d}^{SC} = b_{d\,sum} S_{eff}^{SC}(\Delta n). \qquad (28)$$

Comparing the values (26) and (27) with each other, the following differences should be noted. First, due to the fact that $S_{eff\,d}^{SC}$ is larger than $S_{SC}(\Delta n)$, when x_m and σ are large enough, the value of $b_{d\,sum}$ should be slightly less than b_d. However, in the case of sufficiently small x_m and σ, the value of $S_{eff\,d}^{SC}$ will be decreased relatively to $S_{SC}(\Delta n)$, which will lead to an increase in $b_{d\,sum}$. As these calculations show, the second effect dominates in silicon SCs described in [14, 18], *i.e.* the resulting value of $b_{d\,sum}$ increases slightly. However, this effect is relatively small and in the relevant range of not too large Δn it is about 10%.

The theoretical values obtained using Eq. (28) must be fitted to the experimental curves (symbols in Figs 6 to 8). Our calculations showed that for the case of SC described in [18], agreement between the experimental $S_{SC}(\Delta n)$ data and the theoretical equation (28) is achieved for $\tau_{Rm} = 8.4\cdot10^{-6}$ s, $b_r = 0.1$, $x_m = 1.8\cdot10^{-5}$ cm, $\sigma = 1.5\cdot10^{-5}$ cm, and $d_{eff} = 8.3\cdot10^{-5}$ cm (see Fig. 6).

The curves S_{effd}^{SC} *vs.* Δn built in the interval from 10^8 to 10^{17} cm^{-3} by using Eqs (28) and (24) are represented by the curves *1* and *2*, respectively. The curve *3* shows the SCR recombination velocity given by the following expression:

$$S_w^{SC}(\Delta n) = \int_0^{w(\Delta n)} \frac{\tau_{Rm}^{-1} \exp\left(-\frac{(x-x_m)^2}{2\sigma^2}\right)(n_0+\Delta n)\,dx}{(n_0+\Delta n)e^{y(x)} + b_r(p_0+\Delta n)e^{-y(x)}}, \qquad (29)$$

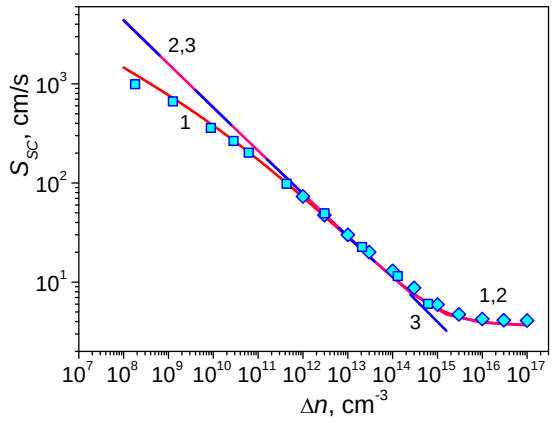

Fig. 6. Experimental dependence of $S_{SC}(\Delta n)$ (symbols). The theoretical curves *1* and *2* for the case when $\tau_{Rm} = 8.3\cdot10^{-6}$ s, $b_r = 0.1$, $x_m = 1.8\cdot10^{-5}$ cm, $\sigma = 1.5\cdot10^{-5}$ cm, $d_{eff} = 8.35\cdot10^{-5}$ cm are obtained using the data given in [18]. The curve *3* describes the SCR recombination velocity without account of the contribution of initial part in the SCR that has become neutral.

which does not account for the contribution of that initial part of the SCR that became neutral. As can be seen from the comparison of curves *2* and *3*, at $\Delta n > 10^{14}$ cm^{-3} the curves diverge, and at $\Delta n = 10^{16}$ cm^{-3} the value of S_{eff}^{SC} is equal to 3.9 cm/s, while the value of S_w^{SC} is 1.14 cm/s. *I.e.*, their difference describes the contribution of this SCR part, that has become neutral, and is equal to 2.76 cm/s. At $\Delta n \geq 10^{15}$ cm^{-3}, the function $S_{eff}^{SC}(\Delta n)$ tends to saturate, while $S_w^{SC}(\Delta n)$ continues to decrease with a slope close to 0.5.

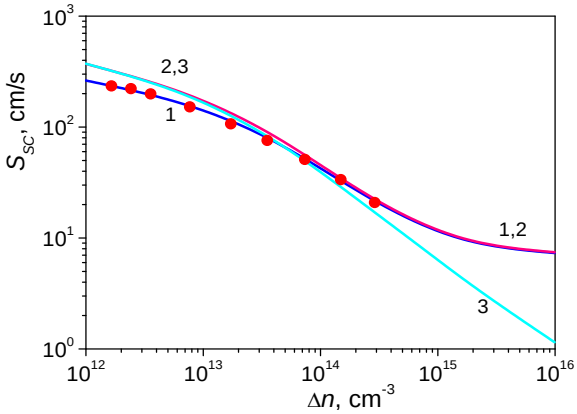

Fig. 7. The SCR recombination velocity $S_{SC}(\Delta n)$ obtained using the experimental data of [14]. Symbols indicate the experimental data. The curves *1* and *2* are, respectively, the theoretical S_{eff}^{SC} and $S_{eff\,d}^{SC}$ plots. The curve *3* represents SCR recombination velocity obtained without account of the part of SCR that has become neutral. The theoretical curves are obtained with the following parameter values: $\tau_{Rm} = 2.5\cdot10^{-7}$ s, $b_r = 50$, $x_m = 3\cdot10^{-5}$ cm, $\sigma = 5\cdot10^{-5}$ cm, $d_{eff} = 2.47\cdot10^{-4}$ cm.

Fig. 7 shows the experimental (symbols) and theoretical (curves) results for the SCR recombination velocity, obtained for the materials described in [14]. The curves *1* and *2* are obtained using Eqs (28) and (24), respectively. Agreement between experiment and theory was achieved using the following parameters: $\tau_{Rm} = 2.5\cdot10^{-7}$ s, $b_r = 50$, $x_m = 3\cdot10^{-5}$ cm, $\sigma = 5\cdot10^{-5}$ cm, $d_{eff} = 2.47\cdot10^{-4}$ cm. The curves *2* and *3* exhibit similar trends as in the case analyzed in Fig. 6.

Finally, let us use the procedure described above to find the experimental value of S_{SC} and its dependence on the excess concentration of charge carriers for the SC with record photoconversion efficiency described in the work of Yoshikawa *et al*. [19]. In our work [27], we have already theoretically modeled the key characteristics of this SC, with account of recombination in SCR. In order to perform the procedure described above for finding the experimental value of the recombination rate in SCR, we used Fig. 4b from [19] and the following parameters obtained by fitting the theoretical dependence (23) in [27]: $\tau_{Rm} = 1.4\cdot10^{-5}$ s, $b_r = 0.1$, $x_m = 2.5\cdot10^{-5}$ cm, $\sigma = 4.5\cdot10^{-6}$ cm, $d_{eff} = 4.18\cdot10^{-5}$ cm.

The curves *2* and *3* behave similar to the case from Fig. 6. Fig. 8 shows the experimental and theoretical relations obtained using formulas (28) and (24), curves *1* and *2*, respectively. As can be seen from the figure, at $\Delta n > 10^{14}$ cm^{-3}, the experimental and theoretical dependences of S_{SC} calculated in different approximations, completely coincide. This is due to the large values of τ_{Rm} in this case and the lower-bounded experimental value Δn of the order of 10^{14} cm^{-3}, which was realized in [19].

The general conclusion that can be drawn analyzing Figs 6–8 is that within the excess concentration range $\Delta n > 10^{14}$ cm^{-3}, the contribution of bulk recombination in that part of SCR, which has become neutral, exceeds the contribution of recombination in SCR itself and must be taken into account in the calculations of S_{eff}^{SC}. The obtained results also indicate that the Gaussian distribution of the inverse SCR lifetime satisfactorily describes the experimental distribution of deep levels in the SCR of these SCs, as evidenced by the good agreement between theoretical curves and experimental data.

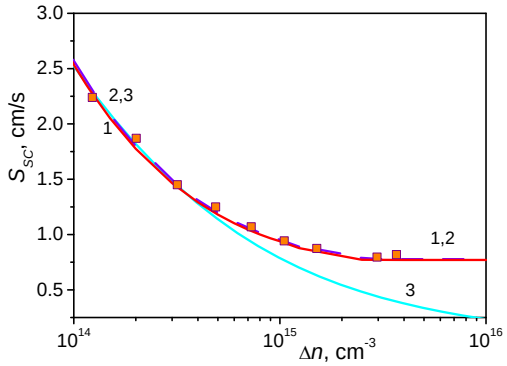

Fig. 8. Symbols: experimental SCR recombination velocity $S_{exp}(\Delta n)$. The theoretical curves *1* and *2* have been obtained using the data given in the work [17] based on the formulas (28) and (24) with $\tau_{Rm} = 1.4\cdot10^{-5}$ s, $b_r = 0.1$, $x_m = 2.5\cdot10^{-5}$ cm, $\sigma = 4.5\cdot10^{-6}$ cm, $d_{eff} = 4.18\cdot10^{-5}$ cm. The curve *3* describes the SCR recombination velocity without accounting for that initial part of the SCR that has become neutral.

It should be noted that despite the fact that the value of the effective recombination velocity in the SCR in this case is small, due to its very slow decline in the vicinity of the maximal photoconversion efficiency, it can play a significant role along with other recombination processes and affect the value of the photoconversion efficiency. This will be discussed in more detail in the next section.

4. The effect of $\Delta n(x)$ dependences associated with a high SCR recombination velocity on the effective lifetime of excess charge carriers in the base of the barrier structure

The effective lifetime of excess charge carriers is an important characteristic of the quality of silicon barrier structures and its research has been quite intensive among scientists who are engaged in the development of silicon SCs and are looking for ways to increase their efficiency. There are several approaches to its determination, and one of them, as shown in a number of works, consists in studying the dependence of the short-circuit current on the open-circuit voltage [18, 19]. From the physical viewpoint, the study of $J_L(V_{OC})$ dependences is similar to the study of dark *I–V* curves and provides information about the SCR recombination. Their only difference is that $J_L(V_{OC})$ curves, in contrast to dark *I–V* curves, do not contain information about series resistance.

Unfortunately, today there are few works, with the exception of [18, 20], in which studies of $J_L(V_{OC})$ dependences were performed in a wide range of illumination intensities, starting from values when V_{OC} is low. In the work of Cuevas and Kerr [20], the interpretation of the obtained results was carried out using a simplified approach based on the use of two-exponential *I–V* curves, one of them was considered to be the contribution from SCR recombination with an assumed ideality factor of 2. In our work [18], the interpretation of the results of the study of the SunPower SCs with reverse metallization was performed in a more general form. In [19], these dependences, or rather, the dependences of illumination on the open-circuit voltage, were measured starting from V_{OC} values equal to 0.53 V.

The short-circuit current of some SC with a unit area can be written as [18]

$$I_L = \frac{qd}{\tau_{eff}(\Delta n_{OC})}\Delta n_{OC} + \frac{V_{OC}}{R_{SH}}\ , \qquad (30)$$

where

$$\Delta n_{OC} = -\frac{n_0}{2} + \sqrt{\frac{n_0^2}{4} + n_{i0}^2 e^{\Delta E_g/kT}\left(e^{qV_{OC}/kT} - 1\right)}\ . \qquad (31)$$

Here, n_{i0} is the intrinsic concentration in the absence of the bandgap narrowing effect, and ΔE_g is its value [21]. The dependence of the dark current on the applied voltage is similar to the expression (30):

$$I_D(V) = \frac{qd\ \Delta n}{\tau_{eff}(\Delta n)} + \frac{V - IR_s}{R_{SH}}. \quad (32)$$

The only difference between these two expressions is that $I_D(V)$ depends on the series resistance R_S. It follows from (32) that

$$\tau_{eff} = \frac{J_L(V_{OC}) - \dfrac{V_{OC}}{R_{SH}}}{qd\Delta n_{OC}}. \quad (33)$$

For further calculations, we will need a theoretical expression for the effective lifetime in silicon $\tau_{eff}(\Delta n)$. The net lifetime is formed by intrinsic and extrinsic recombination mechanisms,

$$\tau_{eff}^{-1} = \tau_{intr}^{-1} + \tau_{extr}^{-1}, \quad (34)$$

where the intrinsic lifetime τ_{intr} is formed by the radiative and Auger band-to-band recombination (see [19, 22–25]), and the extrinsic lifetime τ_{extr} is formed, by SRH recombination, the non-radiative exciton Auger recombination assisted by deep impurities, surface recombination, and SCR recombination. Denoting the lifetimes associated with these processes, respectively, as τ_{SRH}, τ_{eff}^{b}, τ_{eff}^{s}, and τ_{scr}, we can write

$$\tau_{extr} = \left(\left(\tau_{eff}^{b}\right)^{-1} + \tau_{SRH}^{-1} + \left(\tau_{eff}^{s}\right)^{-1} + \left(\tau_{scr}\right)^{-1}\right)^{-1}. \quad (35)$$

The effective bulk lifetime of charge carriers in the base region τ_{eff}^{v}, discussed earlier, is defined as

$$\tau_{eff}^{v} = \left(\tau_{eff}^{b}\right)^{-1} + \tau_{SRH}^{-1} + \tau_{intr}^{-1}. \quad (36)$$

The value of SRH lifetime depending on the doping level and the excitation level in a *n*-type semiconductor is described by the expression

$$\tau_{SRH} \cong \tau_{p0}\frac{\tau_{p0}(n_0 + n_1 + \Delta n) + \tau_{n0}(p_1 + \Delta n)}{n_0 + \Delta n}, \quad (37)$$

where $\tau_{p0} = (V_p \sigma_p N_t)^{-1}$, $\tau_{n0} = (V_n \sigma_n N_t)^{-1}$, V_p and V_n are the mean thermal velocities of holes and electrons, σ_p and σ_n are their capture cross sections by the recombination centers of concentration N_t, and n_1, p_1 are the electron and hole concentrations when the Fermi energy coincides with the energy of the recombination center. Depending on the excess concentration of electron-hole pairs, the lifetime τ_{SRH} changes between the low-injection and high-injection extreme values.

The non-radiative exciton Auger recombination lifetime [26] is

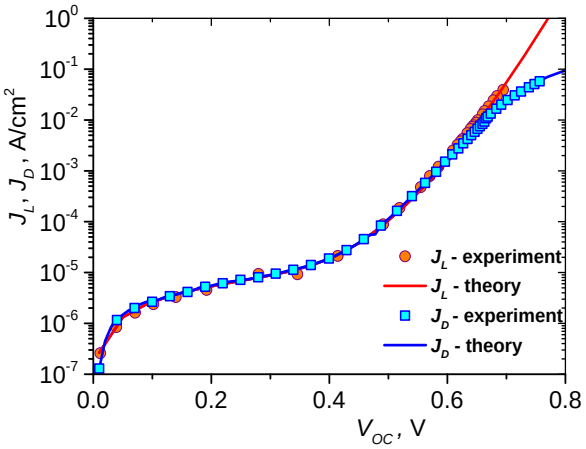

Fig. 9. The dark current density *vs*. applied voltage and the short-circuit current density *vs*. the open-circuit voltage, as obtained in [14]. The symbols indicate the experimental data, the lines represent the theoretical curves.

$$\tau_{eff}^{b} = \tau_{SRH}\frac{n_x}{n_0 + \Delta n}, \quad (38)$$

where $n_x = 8.2 \cdot 10^{15}$ cm^{-3}. In the appendix, the history of the appearance of this lifetime is considered in detail, the necessity of its use is substantiated, its place among other times is established, and its manifestation in silicon barrier structures with long lifetimes is illustrated on a concrete example.

For the Auger interband recombination lifetime, we used the empirical expression given in [23].

The surface recombination lifetime is

$$\tau_{eff}^{s} = d/S_s, \quad (39)$$

where S_s is the total recombination velocity on the front and back surfaces.

Next, we specify the dependence of the surface recombination velocity on the level of excitation and on the level of doping. We will assume that the value is defined by the expression

$$S_s = S_{0s}\left(\frac{n_0}{n_p}\right)^m\left(1 + \frac{\Delta n}{n_0}\right)^r, \quad (40)$$

where S_{0s} is the total value of surface recombination velocity on the front and back surfaces at a low level of excitation, n_p is the initial value of the doping level, $m \approx 1$, and the value of r for most silicon samples is also equal to unity. The lifetime due to recombination in SCR is defined as

$$\tau_{SCR} = \left(\frac{S_{SCd}}{d}\right)^{-1}. \quad (41)$$

Now we will return to the interpretation of the results of the $J_L(V_{OC})$ measurements, taking into account the results of the first section in this paper, *i.e.*, using the

$S_{SCd}(\Delta n)$ dependences. Fig. 9 shows the experimental curves $J_L(V_{OC})$, combined with the $J_D(V)$ curves for one of the SCs studied in [18]. As can be seen from the figure, they coincide up to $V_{OC}(V)$ values of 0.65 V, and diverge at higher values. They were calculated theoretically within the approach used in this work, when the expression (2) was used once for the dependences of the recombination rate in SCR, and the second time the expression $S_{SCd}(\Delta n)$ was applied.

Visually, there are no differences in the $J_L(V_{OC})$ and $J_D(V)$ curves calculated in the first and second approximation. However, the theoretical dependences of $\tau_{eff}(\Delta n)$ obtained using the $J_L(V_{OC})$ curves are shown in Fig. 7. At the values of Δn less than 10^{14} cm^{-3}, they differ. The smaller the value of Δn, the larger their difference. The obtained result is consistent with the theory developed in the first chapter. The $\tau_{eff}(\Delta n)$ values calculated using the $S_{SCd}(\Delta n)$ dependences are larger.

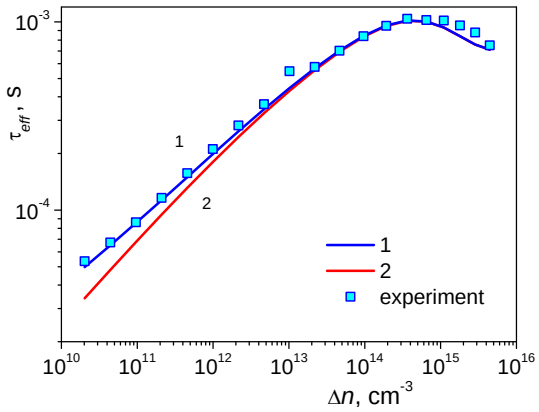

Fig. 10. Effective lifetime in silicon *vs.* the excitation level obtained theoretically with and without taking into account the change in the SCR recombination velocity in the presence of a concentration gradient (*1* and *2*) and the experimental data plotted when being based on the values of τ_R and b_r from [14].

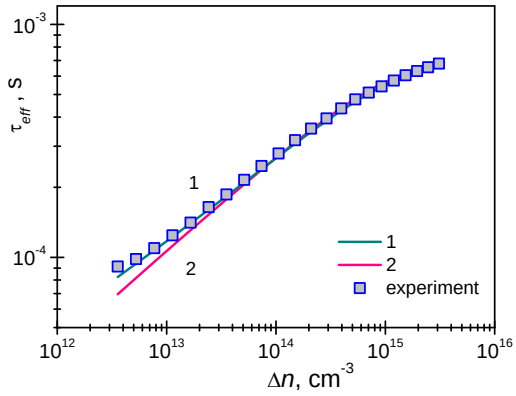

Fig. 11. Effective lifetime in Si SC base *vs.* the excitation level, as obtained with and without taking into account the variation of the SCR recombination velocity in the presence of the concentration gradient (*1* and *2*) and the respective experimental curve obtained using the results and the values for τ_R and b_r from [18].

Fig. 10 also shows the experimental $\tau_{eff}(\Delta n)$ curves obtained using the experimental values of $J_L(V_{OC})$. As can be seen from the figure, it is in good agreement with the theoretical dependence calculated using the $S_{SCd}(\Delta n)$ formula. A procedure similar to that used above was applied in processing the dependences of the dark current on the applied voltage, measured in our work [14]. Theoretical curves of the effective lifetimes were constructed with and without taking into account the dependences of the SCR recombination velocity $S_{SC}(\Delta n)$ on the calculated effect. They are shown in Fig. 11. It also shows the experimental dependence of $\tau_{eff}(\Delta n)$ using the experimental values of $J_D(V)$ measured in this work, at the voltage values lower than 0.6 V, when the dark *I–V* characteristic coincides with the $J_L(V_{OC})$ dependence. As can be seen from the figure, at Δn less than 10^{15} cm^{-3}, which corresponds to the voltage less than 0.6 V, it is consistent with the theoretical dependence that takes into account the calculated effect, *i.e.* the experimental values of $\tau_{eff}(\Delta n)$ are larger.

5. The effect of SCR recombination on the characteristics of highly efficient silicon solar cells

Theoretical estimates, which are based on the assumption that the SCR recombination time in silicon solar cells are close to the SRH recombination time in the base, lead to the conclusion that the SCR recombination in silicon SCs should not affect their characteristics, unlike silicon diodes. This is due to the fact that the main characteristics of SC, such as photoconversion efficiency, open-circuit voltage and others, are determined by their operation in the region of sufficiently large characteristic concentrations of excess electron-hole pairs under conditions of maximum extracted power and under conditions of open circuits. In this range of excess concentrations of charge carriers (of the order of 10^{15} to 10^{16} cm^{-3}), according to estimates by using the above assumption at $\tau_R = 10^{-3}$ s according to expression (2), the value of $S_{SC}(\Delta n)$ in the order of magnitude is equal to 0.01 cm/s, *i.e.*, it is significantly smaller than other recombination components.

However, the reality was not so optimistic. It was found that, as mentioned earlier, the recombination times in SCR were significantly shorter, of the order of 10^{-4} to 10^{-7} s. The reasons for this are not always clear, especially in the case of HIT elements, in the manufacture of which high temperatures are not used. Estimation of the values of $S_{SC}(\Delta n)$ and $S_{SCw}(\Delta n)$ at $\tau_R = 10^{-7}$ s gives values of the order of 150 and 100 cm/s, which, as a rule, significantly exceeds the recombination contributions from other recombination mechanisms. Therefore, we will further calculate the effect of recombination in SCR on the parameters of highly efficient silicon SCs depending on the value of τ_R. Furthermore, as can be seen from Figs 6–8, in the range $\Delta n \geq 10^{15}$ cm^{-3}, the contribution of bulk recombination in that part of SCR, which has become neutral, is added to the net SCR recombination velocity. Therefore, we will further calculate the effect

Table. Key parameters of highly efficient silicon SCs for various values of SCR lifetime.

τ_R, s	10^{-3}	10^{-4}	10^{-5}	10^{-6}	10^{-7}
η, %	24.0	24.0	23.5	21.6	18.6
V_{OC}, V	0.705	0.705	0.704	0.692	0.626
Δn_m, cm^{-3}	$1.74\cdot10^{15}$	$1.69\cdot10^{15}$	$1.39\cdot10^{15}$	$5.47\cdot10^{14}$	$3.02\cdot10^{13}$
Δn_{OC}, cm^{-3}	$6.86\cdot10^{15}$	$6.84\cdot10^{15}$	$6.65\cdot10^{15}$	$5.1\cdot10^{15}$	$1.13\cdot10^{15}$

of recombination in SCR on the parameters of highly efficient silicon SCs depending on the τ_R value, taking this into account. For this, we will need the theoretical expressions for all recombination components in silicon given in the third chapter.

Using the theoretical approach from [18], the *I–V* relation in the presence of illumination,

$$I(V) = I_L - \frac{qd\ \Delta n}{\tau_{eff}(\Delta n)} + \frac{V + IR_s}{R_{SH}}, \qquad (42)$$

allows one to find such fundamental characteristics of silicon SCs as photoconversion efficiency under AM1.5 conditions and open-circuit voltage. We will obtain their dependence on the SCR recombination lifetime with the following parameters: $\tau_{SRH} = 10^{-2}$ s, $d = 150$ μm, $T = 298$ K, $n_0 = 10^{15}$ cm^{-3}, $R_S = 0.3$ Ohm·cm^2, $R_{SH} = 3\cdot10^4$ Ohm·cm^2.

First, let's analyze the case when the value of $b_r \geq 1$. The calculation results are shown in Table. To produce these data, it was assumed that $b_r = 1$. The same table shows the values of the excess concentrations Δn_m and Δn_{OC}, which are equal to the values of the excess concentration at the points of maximum power collection and in the open-circuit regime.

As can be seen from the table, the effect of recombination in SCR on the photoconversion efficiency is greater than its effect on the open-circuit voltage. And this is understandable, because the excess concentration in open-circuit regime exceeds the concentration of excess charge carriers under the condition of maximum extracted power. At the same time, the value of the recombination velocity in SCR is lower and therefore its influence on the open-circuit voltage is less. The effect of SCR recombination on the photoconversion efficiency depending on the value of the SCR lifetime at $\tau_R = 10^{-3}$ s is absent, at $\tau_R = 10^{-4}$ s it is weak, at $\tau_R = 10^{-5}$ s it is moderate, at $\tau_R = 10^{-6}$ s it is strong, and at $\tau_R = 10^{-7}$ s it is extremely high.

It should be also noted that Δn_m in this case is significantly decreased, which correlates with a decrease in the photoconversion efficiency due to an additional increase in the SCR recombination velocity.

In all the cases, except when $\tau_R = 10^{-7}$ s, in the maximum power regime, the gradient effects considered in this paper are insignificant. In the case when $\tau_R = 10^{-7}$ s and $\Delta n_m = 4.7\cdot10^{13}$ cm^{-3}, the value of S_{SC} is 794, and the value of S_{SCd} is 480 cm/s, *i.e.*, the gradient effect is already fully manifested.

If we compare the values for τ_R obtained in Section 4 for SCs described in [14] and [18] with the data in the Table, it can be seen that they correspond to a strong and moderate effect of SCR recombination on photoconversion efficiency.

We will analyze the case when $b_r < 1$ by using the example adduced in [19]. In this work, the value of photoconversion efficiency of 26.6% was obtained. The maximum power selection point in this case was at $\Delta n = 3\cdot10^{15}$ cm^{-3}. At this point, the SCR recombination velocity according to Fig. 11 is 0.8 cm/s, and the sum of all other velocities, as shown by the calculation using the parameters given in the previous section, is 2.63 cm/s. Thus, they are of the same order of magnitude, taking this into account, the rate of recombination in SCR in this case should affect the efficiency of photoconversion. Calculation of the photoconversion efficiency of this SC in the absence of recombination in SCR gives the value 26.9%, which is 1% higher than the achieved value. Thus, in the case when the ratio $b_r < 1$, the recombination in SCR affects the photoconversion efficiency of highly efficient silicon SCs more strongly than when $b_r \geq 1$, even in the case of not too small values of τ_R.

The paper also contains two appendices. In the first appendix, some issues related to SCR recombination are considered in more detail. In the second appendix, a detailed analysis of the problem related to the need to take into account, among the recombination mechanisms in silicon, the non-radiative excitonic Auger recombination mediated by deep impurities, is performed.

6. Conclusions

The main result of this work is that when fitting the experimental results in silicon barrier structures with long bulk lifetimes, it is necessary to take into account that at sufficiently low excitation levels, high values of the recombination velocity in SCR lead to a spatial dependence of the distribution of the excess concentration of electron-hole pairs in the base regions. This, in its turn, renormalizes the value of the SCR recombination velocity, leading to its decrease. With account of this effect, the ideality factor is no longer a constant close to 2, but becomes a function that depends on several parameters and varies within a rather broad range (from ca. 1.3 to 1.8) depending on the value of the SCR lifetime. In this work, the calculations were performed under the assumption that the SRH lifetimes in the base regions are

sufficiently large and greater than a millisecond, which leads to constant values of the excess concentration in these regions at small values of surface and SCR recombination velocities.

The paper shows that the manifestation of this effect leads to an increase in the effective lifetime of excess charge carriers at low values of the excess concentration. Theoretical calculations were confirmed experimentally.

A method is proposed and implemented to determine the SCR recombination velocity from experimental data on silicon barrier structures. A comparison with the theory was carried out, which showed that in the region of sufficiently low values of Δn, the limitation of the SCR recombination velocity is in agreement with the considered effect.

It is shown that due to the decrease in the SCR thickness with Δn, a part of the initial SCR becomes quasi-neutral, and in this region bulk recombination occurs with the lifetime τ_R. Due to the small SCR lifetimes (≤ 1 μs) in real silicon p^+-n-n^+ structures, the value of this recombination velocity S_r can exceed the recombination velocity S_{SC} in SCR, which is determined by the expression (2). It happens at sufficiently large values of Δn. Therefore, in the general case, the effective SCR recombination velocity is defined by their sum, *i.e.*, $S_{eff}^{SC} = S_{SC} + S_r$.

Specific assessments of the impact of SCR recombination on the key characteristics of high-efficiency silicon solar cells, in particular, on the photoconversion efficiency and open-circuit voltage, have been made, and it has been shown that this effect must be taken into account, if the values of the lifetime in the SCR are of the order of less than 10^{-5} s; the lifetimes of this order of magnitude and even shorter are typical for silicon SCs.

It has been shown that the cases when $b_r \geq 1$ and $b_r < 1$ should be considered separately. In the latter case, the effect of SCR recombination on the efficiency of photoconversion is stronger than in the former case.

In addition to the questions above, a detailed analysis of the problem related to the need to take into account the non-radiative exciton Auger recombination with the participation of deep impurities is performed in the appendix. First, its origin and its place alongside other recombination mechanisms are described retrospectively, and then a comparison of the theoretical dependences for the effective lifetime in the silicon bulk with the experiment is made. It confirms the importance of the non-radiative exciton recombination mechanism.

In conclusion, we note that the experimental dependences of the recombination rate in SCR on the excess concentration of electron-hole pairs are in good agreement with the theoretical ones calculated under the assumption of a Gaussian distribution of deep recombination centers in SCR, not only for the SC considered in this work, but also for the SC with a *p-n* junction, studied in [36] and simulated in [37]. It is interesting that the minimum value of lifetimes in SCR are small (of the order of 10^{-5} to 10^{-6} s) occur not only in SCs with a *p-n* junction, but also in heterostructures α-Si:H/Si.

Appendix 1

The electroneutrality equation (5) is obtained under the assumption that there is no hole degeneration in the base region of silicon near the p^+-contact. However, in the case when the surface charge concentration of acceptors N exceeds 10^{12} cm^{-3}, holes may be degenerate in the near-surface part of the base region.

Then, the electroneutrality equation must be formulated taking degeneracy into account

$$N = \left(\frac{2kT\varepsilon_0\varepsilon_{Si}}{q^2} \right)^{1/2} \left[N_V F_{3/2}(y_{0w} + \varepsilon) \right]^{1/2}, \qquad (1A)$$

where the Fermi–Dirac function is defined by

$$F_{3/2}(y_{0w}) = \frac{4}{3\sqrt{\pi}} \int_0^\infty \frac{\varepsilon^{3/2} d\varepsilon}{1 + \exp(y_{0w} + \varepsilon) N_V / p_0}. \qquad (2A)$$

Here, N_V is the effective density of states in the valence band, and p_0 the equilibrium hole concentration in the bulk of base region.

Plotted in Fig. 1A is the dependence of the non-equilibrium dimensionless potential y_s on the surface of the silicon base region bordering with the p^+-contact on the excess concentration of electron-hole pairs Δn for the cases when the value of N is 10^{12} and 10^{13} cm^{-3}, using equations (5), (1A) and (2A). As can be seen from the figure, the $y_s(\Delta n)$ curves, calculated with and without taking into account degeneracy at $N = 10^{12}$ cm^{-2} (curves *1* and *2*), practically coincide, which indicates the absence of degeneracy. As shown by the calculation of the value of surface concentration inherent to holes at the interface with the p^+-contact, it is about $3 \cdot 10^{18}$ cm^{-3}, which is almost an order of magnitude lower than the value of N_V, which at room temperature is $1.8 \cdot 10^{19}$ cm^{-3}. In Fig. 1A, the dependences of non-equilibrium dimensionless potential $y_s(\Delta n)$ are also plotted for the case when the value of N is 10^{13} cm^{-3}. In this case, the curves plotted with (curve *3*) and without (curve *4*) consideration of degeneracy differ.

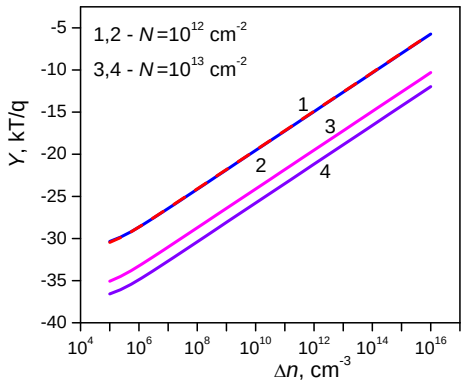

Fig. 1A. The non-equilibrium dimensionless potential y_s on the surface of the silicon base region *vs.* excess concentration of electron-hole pairs Δn at $N = 10^{12}$ cm^{-3} (*1*, *2*) and $N = 10^{13}$ cm^{-3} (*3*, *4*). The curves *1* and *3* were calculated without and curves *2* and *4* with taking degeneracy into account.

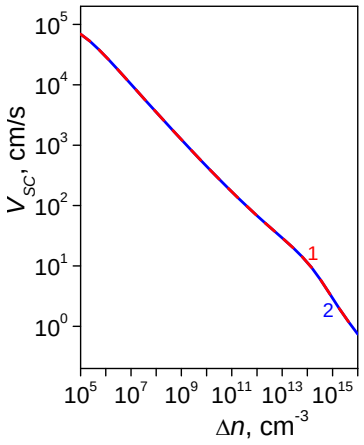

Fig. 2A. SCR recombination velocity *vs*. excess carriers concentration, obtained using Eqs (5) та (1A).

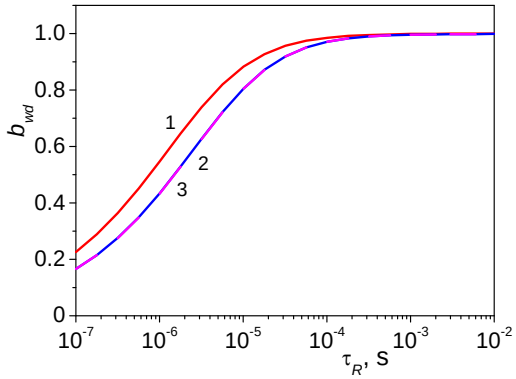

Fig. 3A. The dependence of b_{wd} on τ_R, obtained using Eqs (3A) and (15).

However, the values of the SCR recombination velocities calculated using the equation (2) and their dependence on the excess concentration of charge carriers coincide both at $N = 10^{12}$ cm^{-3} and at $N = 10^{13}$ cm^{-3}, both with and without account of degeneracy (see Fig. 2A). This is related to the fact that the depletion layer, in which the recombination times for holes and electrons either coincide or differ not very much, makes the greatest contribution to SCR recombination.

In a general case, to find the coefficients b_{wd} and b_{w0}, it is necessary to solve the generation-recombination equation, with account that the generation term of the equation is proportional to $e^{-\alpha x}$, where α is the absorption coefficient. When using all the equations given in the main text of the work, taking into account the specified term, we obtain the following expression for $b_{wd}(\alpha)$:

$$b_{wd}(\alpha)=\frac{2+2\left(\frac{S_{SC}}{\alpha D}-1\right)\cosh\left(\frac{d}{L}\right)e^{-\alpha d}-\left(\frac{1}{\alpha L}\frac{S_{SC}L}{D}-1\right)e^{\frac{-d}{L}-\alpha d}-\left(\frac{1}{\alpha L}\frac{S_{SC}L}{D}+1\right)e^{\frac{d}{L}-\alpha d}}{2\left(\frac{S_{SC}}{\alpha D}-1\right)e^{-\alpha d}+2\cosh\left(\frac{d}{L}\right)+2\frac{S_{SC}L}{D}\sinh\left(\frac{d}{L}\right)-\left(\frac{1}{\alpha L}\frac{S_{SC}L}{D}-1\right)e^{-\frac{d}{L}}-\left(\frac{1}{\alpha L}\frac{S_{SC}L}{D}+1\right)e^{\frac{d}{L}}}. \quad (3A)$$

It should be noted that the quantum efficiency of the short-circuit current in textured silicon SCs is determined by an expression of the type

$$q(\lambda,d,b)=\frac{\alpha(\lambda)}{1+\frac{b}{4n_r^2(\lambda)d}}, \quad (4A)$$

and not by

$$q(\lambda,d)=1-\exp(-\alpha(\lambda)d). \quad (5A)$$

Therefore, when obtaining the dependences of $b_{wd}(\alpha)$ for textured silicon SCs, it is necessary to select an effective value of α, which allows one to achieve agreement with experiment based on the use of quantum efficiency (5A) instead of (4A) when finding the short-circuit current in AM1.5 conditions. As the estimates show, the so-obtained typical value of the absorption coefficient α in textured silicon SCs with an efficiency of the order of 20% or higher is approximately $1.1\cdot10^4$ cm^{-1}. Shown in Fig. 3A are the dependences of $b_{wd}(\tau_R)$ for the cases when the value of α is close to zero (at the same time, the generation term in the original equation is a constant), when the value of $\alpha = 1.1\cdot10^4$ cm^{-1}, and according to formula (15) for b_{dw}.

As the calculations show, in the case when $\alpha \approx 0$, the value of $b_{wd}(\tau_R)$ is larger than the value of b_{dw}, obtained according to Eq. (15), but in the case when $\alpha = 1.1\cdot10^4$ cm^{-1}, the values of $b_{wd}(\tau_R)$ and b_{dw} match. The latter case practically corresponds to the surface generation of light in SC.

Let us further consider the important question about the concentration of deep impurities responsible for SCR recombination in those SCs, parameters of which are used in Figs 6 to 8. By definition, in this case the valid ratio is $\tau_R = (C_p N_t)^{-1}$. Let us rewrite it in the following form

$$N_t=\frac{\tau_R^{-1}}{C_n b_r}. \quad (6A)$$

Assume that the value of C_n is constant and equal to 10^{-9} cm^3/c. Then, substituting the values of τ_{Rm} and b_r, for which Figs 6 to 8 were plotted, we obtain, respectively: $N_{tm1} = 1.2\cdot10^{15}$ cm^{-3}, $N_{tm2} = 8\cdot10^{13}$ cm^{-3} and $N_{tm3} = 7.14\cdot10^{14}$ cm^{-3}. If we recalculate the obtained values of deep-level concentrations for the studied SCs by using their Gaussian distribution in SCR, we get $N_1 = 4\cdot10^{10}$ cm^{-2}, $N_2 = 7.3\cdot10^9$ cm^{-2} and $N_3 = 8.1\cdot10^9$ cm^{-2}, respectively. Despite the fact that the maximum concentrations of deep levels for different SCs differ by more than an order of magnitude, the integral

concentrations differ by no more than one and a half times. It is also surprising that the lowest concentration of levels occurs in SC, where the value of τ_R is the smallest.

Finally, we discuss the question about the criteria that should be used when calculating the SCR recombination velocity based on either the τ_R model or the model with a Gaussian distribution of centers in SCR. The approximation $\tau_R \approx$ const can be used when the integrand in Eq. (1) fits completely into the Gaussian. This case is realized in the region of small and medium excitation levels, as a rule, when $\Delta n < 10^{14}$ cm^{-3}. If the integrand function in (1) goes beyond the Gaussian, then the general formula with the Gaussian (24) should be used. This case is realized at sufficiently high excitation levels, when $\Delta n > 10^{14}$ cm^{-3}.

Appendix 2

The recombination component associated with the non-radiative recombination of excitons on bulk recombination centers by the Auger mechanism is described by expression (38). Let's go back to the history of the issue of this recombination. In papers [28–31], it was shown that in semiconductors, in particular in silicon, at sufficiently large values of Δn, when $\Delta n > n_0$, there are two subsystems, electron-hole and exciton. Recombination, both radiative and non-radiative, occurs both through the electron-hole and exciton channels. There is interaction between these subsystems.

In [28], it was established that depending on the value of the excitation level, there are cases when the presence of excitons can be neglected (low excitation level), when excitons affect the effective lifetime of electron-hole pairs (intermediate excitation), and when excitons define all characteristics (high level of excitation).

Does the presence of an exciton channel affect the characteristics of silicon solar cells? At the excess charge carrier concentration of the order of 10^{15} cm^{-3}, which correspond to the point of maximum power selection, the concentration of excitons, which is proportional to the product *pn*, is significantly lower than the value of Δn. It would seem that excitons should not make a significant contribution to the total recombination. But, as it was shown in the works of Hangleiter [32, 33], the spatial localization of an electron and a hole in an exciton significantly increases the probability of Auger processes, both in the form of direct band-to-band recombination and in the form that involves impurity centers. Therefore, in this case, an intermediate level of excitation is realized. Both the first and second cases were analyzed in the works [32, 33]. At the same time, it was ascertained that the same deep level can provide both recombination according to the SRH mechanism and Auger exciton recombination involving deep centers. In [34], the contribution of excitons to the band-to-band recombination in silicon was taken into account, whereas the work [26] incorporates the contribution of excitons to Auger recombination with the participation of deep impurities. It turned out that the effective bulk lifetime of charge carriers in silicon, if taking into account this contribution, depends on the level of doping according to

$$\tau_{eff}(n_0) = \frac{\tau_{\mathrm{SRH}}}{1+\dfrac{n_0}{8.2\cdot 10^{15}}} \ . \qquad (1B)$$

Well before the paper [26], the work [35] was published, in which a similar empirical expression for the dependence of the effective bulk lifetime on the level of doping was proposed, in which the value $7.1\cdot 10^{15}$ cm^{-3} appeared instead of $8.2\cdot 10^{15}$. In the work [35], the proposed expression was compared for a large number of samples with both electron and hole conductivity and a good agreement between empirical and experimental data was obtained. The difference between the characteristic concentration values has a simple explanation: In the work [26], the obtained dependence was isolated from the interband recombination, whereas in [35] it was not done.

In silicon samples with long SRH lifetimes (longer than a millisecond), the non-radiative exciton recombination mechanism with the lifetime (1A) works together with the SRH channel. Thus, at τ_{SRH} of the order of 10 ms, the time of non-radiative exciton recombination significantly reduces their total value in the range of doping levels from 10^{15} to 10^{16} cm^{-3}. In the samples with the doping concentration of 10^{15} cm^{-3}, this decrease reaches 12%, and in the samples with the doping level of $4.9\cdot 10^{15}$ cm^{-3} it is 60%.

The lifetime of non-radiative exciton recombination is structurally closest to the time of radiative recombination

$$\tau_r^{-1} = B_r \left(n_0 + \Delta n\right) \ , \qquad (2B)$$

where B_r is radiative recombination coefficient. Calculations and comparison of the lifetime of non-radiative exciton recombination and the lifetime of radiative recombination in silicon show that at $\tau_{\mathrm{SRH}} \le 50$ ms the former time is shorter than the latter. Even in the record-breaking efficiency of silicon SCs, the value of τ_{SRH} is of the order of 10 ms. Therefore, it is logical, if one takes into account radiative recombination, another also take into account non-radiative exciton recombination.

To confirm this statement, shown in Fig. 1B are the dependences of the effective bulk lifetime for *n*-Si samples with long SRH lifetimes on the doping level, taken from Richter's work [23]. Assuming that the expression (1B) is valid, and that for this reason the experimental points within the range from 10^{15} up to $5.3\cdot 10^{15}$ cm^{-3} are lower, we obtained corrected values that take into account only the influence of radiative recombination and band-to-band recombination, by multiplying the given values by the factor $(1 + n_0/8.2\cdot 10^{15}$ cm$^{-3})$ (blue curve *2*). The use of theoretical dependences that take into account SRH

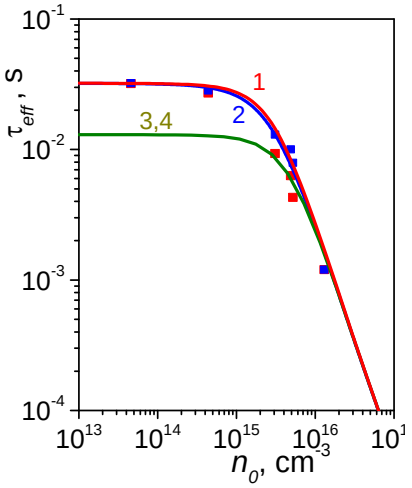

Fig. 1B. Experimental effective lifetime τ_{eff} in silicon *vs* the doping level, taken from [23] (symbols), and theoretical dependences obtained with (*1* and *2*) and without (*3* and *4*) the non-radiative exciton recombination (lines).

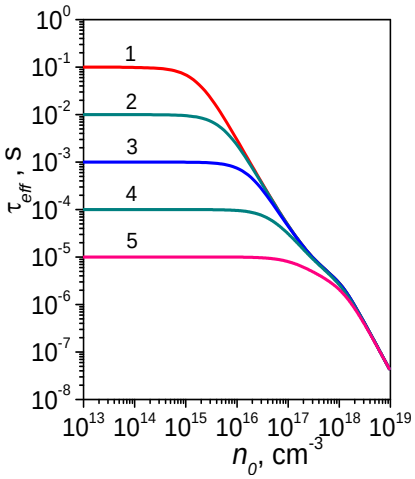

Fig. 2B. Theoretical effective lifetime τ_{eff} in silicon *vs* the doping level at various SRH lifetimes τ_{SRH} = 10^{-1} (*1*), 10^{-2} (*2*), 10^{-3} (*3*), 10^{-4} (*4*), and 10^{-5} s (*5*), obtained with account of the lifetime inherent to non-radiative exciton recombination (lines).

recombination, non-radiative exciton recombination, radiative recombination, and band-to-band Auger recombination enabled to reconcile the corrected experiment with theory. At the same time, the calculation, which does not take into account the non-radiative exciton recombination, does not agree with the experiment (see the red curve*1*).

Fig. 2B shows the dependence of theoretical effective lifetime τ_{eff} in silicon on the doping level at various SRH lifetimes τ_{SRH} obtained with account of the lifetime inherent to non-radiative exciton recombination.

The lifetime is defined by the SRH mechanism and the non-radiative exciton recombination time. So, for example, at the value of τ_{SRH} equal to 10^{-5} s, this range continues up to the values of n_0 that exceed 10^{17} cm^{-3}.

It should be noted that in [30] excitonic non-radiative recombination was actually taken into account by using the lifetime given in [35].

Thus, the excitonic nonradiative recombination must always be taken into account as a separate recombination channel.

References

1. Sah C.T., Noyse R.N., Shockley W. Carrier generation and recombination in *p-n* junctions and *p-n* junction characteristics. *Proc. IRE*. 1957. **45**. P. 1228–1243. http://dx.doi.org/10.1109/JRPROC.1957.278528.
2. Moll J.L. The evolution of the theory of the current-voltage characteristics of *p-n* junctions. *Proc. IRE*. 1958. **46**. P. 1076–1084.
3. Gummel H. K. Hole-electron product of *p-n* junctions. *Solid-State Electron.* 1967. **10**, No 3. P. 209–212. http://dx.doi.org/10.1016/0038-1101(67)90075-5.
4. Choo S.C. Carrier generation-recombination in the space-charge region of an asymmetrical *p-n* junction. *Solid-State Electron.* 1968. **11**, No 11. P. 1069–1077. https://doi.org/10.1016/0038-1101(68)90129-9.
5. Choo S.C. Analytical approximations for an abrupt *p-n* junction under high-level conditions. *Solid-State Electron.* 1973. **16**, No 7. P. 793–799. https://doi.org/10.1016/0038-1101(73)90176-7.
6. Choo S.C. Theory of a forward-biased diffused-junction *p-L-n* rectifier – II. Analytical approximations. *Solid-State Electron.* 1973. **16**, No 2. P. 197–211. https://doi.org/10.1016/0038-1101(73)90030-0.
7. Choo S.C. Theory of a forward-biased diffused-junction *p-L-n* rectifier – part III: Further analytical approximations. *IEEE Trans. Electron Devices.* 1973. **ED-20**, No 4. P. 418–426. https://doi.org/10.1109/T-ED.1973.17664.
8. Barybin A.A., Santos E.J. P. A unified approach to the large-signal and high-frequency of *p-n* junctions. *Semicond. Sci. Technol.* 2007. **22**, No 11. P. 1225–1231. https://doi.org/10.1088/0268-1242/22/11/008.
9. Fahrenbruch A.L., Bube R.H. *Fundamentals of Solar Cells. Photovoltaic Solar Energy Conversion*. New York, Elsevier, 1983. https://doi.org/10.1016/B978-0-12-247680-8.X5001-4.
10. Nussbaum A. Generation-recombination behavior of Si diodes. *phys. status solidi (a)*. 1973. **19**, No 2. P. 441–450. https://doi.org/10.1002/pssa.2210190207.
11. Corkish R., Green M.A. Junction recombination current in abrupt junction diodes under forward bias. *J. Appl. Phys.* 1996. **80**. P. 3083–3090. https://doi.org/10.1063/1.363168.
12. McIntosh K.R., Altermatt P.P., Heiser G. Depletion region recombination in silicon solar cells: When does m_{DR} = 2? 2000. *Proc. 16th European Photovoltaic Solar Energy Conf.*, Glasgow, 1-5 May 2000. P. 251–254. https://doi.org/10.4324/9781315074405.

13. Yamamoto K. 25.1% efficiency Cu metallized heterojunction crystalline Si solar cell. *25th International Photovoltaic Science and Engineering Conference*, Busan, Korea, November, 2015.
14. Sachenko A.V., Kostylyov V.P., Sokolovskyi I.O. *et al*. Specific features of current flow in α-Si:H/Si heterojunction solar cells. *Techn. Phys. Lett.* 2017. **43**. P. 152–155. https://doi.org/10.1134/S1063785017020109.
15. Sachenko A.V., Kostylyov V.P., Vlasiuk V.M. *et al.* Features in the formation of recombination current in the space charge region of silicon solar cells. *Ukr. J. Phys.* 2016. **61.** P. 917–922. https://doi.org/10.15407/ujpe61.10.0917.
16. Dauwe S. Low Temperature Surface Passivation of Crystalline Silicon and Its Application to the Rear Side of Solar Cells. *PhD thesis*, Universität Hannover, 2004.
17. Hollemann C., Haase F., Schäfer S. *et al*. 26.1%-efficient POLO-IBC cells: Quantification of electrical and optical loss mechanisms. *Prog. Photovolt: Res. Appl*. 2019. **26**, No 1. P. 3–958. https://doi.org/10.1002/pip.3098.
18. Sachenko A.V., Kostylyov V.P., Vlasiuk V.M. *et al*. Characterization and optimization of highly efficient silicon-based textured solar cells: Theory and experiment. *2021 IEEE 48th Photovoltaic Specialists Conf. (PVSC).* 20-25 June, 2021. P. 0544–0550. https://doi.org/10.1109/PVSC43889.2021.9518764.
19. Yoshikawa K., Kawasaki H., Yoshida W. *et al*. Silicon heterojunction solar cell with interdigitated back contacts for a photoconversion effciency over 26%. *Nature Energy*. 2017. **2**. P. 17032(1–8). https://doi.org/10.1038/nenergy.2017.3.
20. Kerr M.J., Cuevas A., Sinton R.A. Generalized analysis of quasi-steady-state and transient decay open circuit voltage measurements. *J. Appl. Phys.* 2002. **91**, No 1. P. 399–404. https://doi.org/10.1063/1.1416134.
21. Schenk A. Finite-temperature full random-phase approximation mode of band gap narrowing for silicon device simulation. *J. Appl. Phys.* 1998. **84**. P. 3684–3695. https://doi.org/10.1063/1.368545.
22. Richter A., Glunz S.W., Werner F. *et al*. Improved quantitative description of Auger recombination in crystalline silicon. *Phys. Rev. B.* 2012. **86**. P. 165202 (14p.). https://doi.org/10.1103/PhysRevB.86.165202.
23. Black L.E., Macdonald D.H. On the quantification of Auger recombination in crystalline silicon. *Sol. Energy Mater. Sol. Cells.* 2022. **234**. P. 111428 (15). https://doi.org/10.1016/j.solmat.2021.111428.
24. Niewelt T., Steinhauser B., Richter A. *et al.* Reassessment of the intrinsic bulk recombination in crystalline silicon. *Sol. Energy Mater. Sol. Cells.* 2022. **235**. P. 111467 (13 p.). https://doi.org/10.1016/j.solmat.2021.111467.
25. Fell A., Niewelt T., Steinhauser B. *et al*. Radiative recombination in silicon photovoltaics: Modeling the influence of charge carrier densities and photon recycling. *Sol. Energy Mater. Sol. Cells*. 2021. **230**. P. 111198. https://doi.org/10.1016/j.solmat.2021.111198.
26. Sachenko A.V., Kostylyov V.P., Vlasyuk V.M. *et al*. The influence of the exciton nonradiative recombination in silicon on the photoconversion efficiency. 2016. *32 European Photovoltaic Solar Energy Conf. and Exhib*. P. 141–147.
27. Sachenko A.V., Kostylyov V.P., Vlasyuk V.M. *et al*. Analysis of the recombination mechanisms in silicon solar cells with the record 26.6% photoconversion efficiency. *48th Photovoltaic Specialists Conf.* 20–25 June, 2021. P. 0532–0539. https://doi.org/10.1109/PVSC43889.2021.9519055.
28. Sachenko A.V., Tyagai V.A., Kundzich A.G. Exciton luminescence in semiconductrors. Surface recombination and space charge layer effects. *phys. status solidi (b)*. 1978. **88**, No 2. P. 797–804. https://doi.org/10.1002/pssb.2220880247.
29. Kane D.E., Swanson R.M. The effect of excitons on apparent band gap narrowing and transport in semiconductors. *J. Appl. Phys.* 1993. **73**, No 3. P. 1193–1197. https://doi.org/10.1063/1.353285.
30. Corkish R., Daniel C., Green M.A. Excitons in silicon diodes and solar cells: A three-particle theory. *J. Appl. Phys.* 1993. **79**, No 1**.** P. 195–203. https://doi.org/10.1063/1.360931.
31. Green M. A. Excitons in silicon solar cells: room temperature distributions and flows. *2nd World Conference and Exhibition on Photovoltaic Solar Energy Conversion*, 6–10 July 1998, Vienna, Austria, P. 74–76.
32. Hangleiter A. Nonradiative recombination *via* deep impurity levels in silicon: Experiment. *Phys. Rev. B*. 1987. **35**, No 17. P. 9149–9161. https://doi.org/10.1103/physrevb.35.9149.
33. Hangleiter A. Nonradiative recombination *via* deep impurity levels in semiconductors: The excitonic Auger mechanism. *Phys. Rev.* B. 1988. **37**. P. 2594–2604. https://doi.org/10.1103/physrevb.37.2594.
34. Kerr M.J., Cuevas A. General parameterization of Auger recombination in crystalline silicon. *J. Appl. Phys.* 2002. **91**, No 4. P. 2473–2480. https://doi.org/10.1063/1.1432476.
35. Fossum J.G. Computer-aided numerical analysis of silicon solar cells. *Solid State Electron*. 1976. **19**, No 4. P. 269–277. https://doi.org/10.1016/0038-1101(76)90022-8.
36. Richter A., Benick J., Feldmann F. *et al*. *n*-type Si solar cells with passivating electron contact: Identifying sources for efficiency limitations by wafer thickness and resistivity variation. *Sol. Energy Mater. Sol. Cells*. 2017. **173**. P. 96–105. https://doi.org/10.1016/j.solmat.2017.05.042.
37. Sachenko A., Kostylyov V., Vlasyuk V. *et al*. Optimization of textured silicon solar cells. *47th Photovoltaic Specialists Conf.*, 2020. P. 0719–0793. https://doi.org/10.1109/PVSC45281.2020.9300877.

Authors and CV

Sachenko A.V. Professor, Doctor of Physics and Mathematics Sciences, Chief Researcher at the Laboratory of Physical and Technical Fundamentals of Semiconductor Photovoltaics at the V. Lashkaryov Institute of Semiconductor Physics. He is the author of more than 300 scientific publications. His main research interests include analysis, characterization, and modeling of silicon solar cells.
E-mail: sach@isp.kiev.ua,
https://orcid.org/0000-0003-0170-7625

Evstigneev M.A. Assistant Professor of the faculty of Physics and Physical Oceanography at the Memorial University of Newfoundland. His research areas are non-equilibrium statistical physics, biophysics, surface science.
E-mail: mevstigneev@mun.ca,
https://orcid.org/0000-0002-7056-2573

Kostylyov V.P. Professor, Doctor of Physics and Mathematics Sciences, Head at the Laboratory of Physical and Technical Fundamentals of Semiconductor Photovoltaics at the V. Lashkaryov Institute of Semiconductor Physics. He is the author of 300 scientific publications. The area of his scientific interests includes photovoltaics and betavoltaics, research, analysis and modeling of solar cells, characterization and testing the solar cells, as well as characterization of the optical and recombination properties of photovoltaics materials.
E-mail: vkost@isp.kiev.ua,
https://orcid.org/0000-0002-1800-9471

Authors' contributions

Sachenko A.V.: formulation of the problem, analysis, investigation, data curation (partially), visualization, writing – original draft, writing – review & editing,
Kostylyov V.P.: conceptualization, methodology, validation, analysis, data curation, writing – original draft, writing – review & editing.
Evstigneev M.: analysis, validation, writing – review & editing.

Рекомбінація в області просторового заряду у високоефективних кремнієвих сонячних елементах

А.В. Саченко, В.П. Костильов, М. Євстігнєєв

Анотація. У роботі теоретично розраховано швидкість рекомбінації в області просторового заряду (ОПЗ) у кремнієвих бар'єрних структурах з великими часом життя за механізмом Шоклі–Ріда–Холла з урахуванням градієнта концентрації надлишкових електронно-діркових пар у базових областях при достатньо великих її значеннях. Проаналізовано залежності коефіцієнта неідеальності рекомбінації в ОПЗ у даному випадку від часу життя в ОПЗ та від прикладеної напруги. Показано, що при наявності градієнта концентрації пар величина коефіцієнта неідеальності рекомбінації в ОПЗ істотно зменшується. Установлено, що вказаний механізм забезпечує збільшення ефективного часу життя надлишкових електронно-діркових пар порівняно з випадком, коли він несуттєвий, що реалізується при достатньо низьких значеннях надлишкової концентрації електронно-діркових пар. Запропоновано та реалізовано метод знаходження експериментальної величини швидкості рекомбінації в ОПЗ у високоефективних кремнієвих сонячних елементах з використанням припущення про гауссовий розподіл оберненого часу життя електронно-діркових пар в ОПЗ. Показано, що при достатньо великих надлишкових концентраціях електронно-діркових пар ефективна швидкість рекомбінації в ОПЗ складається з рекомбінації в ОПЗ та об'ємної рекомбінації в області, де відбулося спрямлення зон. Виконано порівняння розвинутої теорії з експериментом та показано, що між ними існує узгодження. З порівняння теорії з експериментом для низки кремнієвих сонячних елементів визначено час життя в ОПЗ та відношення перерізу захоплення дірки до перерізу захоплення електрона. Виконано конкретні оцінки впливу рекомбінації в ОПЗ на ключові характеристики високоефективних кремнієвих сонячних елементів, зокрема на ефективність фотоперетворення та напругу розімкненого кола. Показано, зокрема, що цей вплив визначається не лише часами життя носіїв заряду в ОПЗ, а й відношенням перерізів захоплення дірок до перерізів захоплення електронів σ_p/σ_n. Так, у випадку, коли $\sigma_p/\sigma_n < 1$, цей вплив істотно посилюється, а у випадку, коли $\sigma_p/\sigma_n > 1$, послаблюється. У Додатку 2 детально проаналізовано необхідність урахування в кремнії часу життя безвипромінювальної екситонної Оже рекомбінації за участю глибоких домішок. Показано, зокрема, що його врахування дозволяє узгодити між собою теоретичні та експериментальні залежності для ефективного часу життя в об'ємі кремнію.

Ключові слова: кремнієвий сонячний елемент, швидкість рекомбінації в ОПЗ, напруга розімкненого кола, струм короткого замикання, ефективність фотоперетворення.